

## Room temperature ferromagnetism in HfO<sub>2</sub> films

K. Kamala Bharathi<sup>\*</sup>, S. Venkatesh, G. Prathiba, N. Harish Kumar, and C. V. Ramana

Citation: *J. Appl. Phys.* **109**, 07C318 (2011); doi: 10.1063/1.3559490

View online: <http://dx.doi.org/10.1063/1.3559490>

View Table of Contents: <http://aip.scitation.org/toc/jap/109/7>

Published by the [American Institute of Physics](#)

---

---

## Room temperature ferromagnetism in HfO<sub>2</sub> films

K. Kamala Bharathi,<sup>1,a)</sup> S. Venkatesh,<sup>2</sup> G. Prathiba,<sup>3</sup> N. Harish Kumar,<sup>3</sup> and C. V. Ramana<sup>1</sup>

<sup>1</sup>Department of Mechanical Engineering, University of Texas at El Paso, El Paso, Texas 79968, USA

<sup>2</sup>Department of Condensed Matter Physics and Material Sciences, Tata Institute of Fundamental Research, Homi Bhabha Road, Mumbai 400005, India

<sup>3</sup>Advanced Magnetism and Magnetic Materials Lab (AMMLa), Department of Physics, Indian Institute of Technology, Chennai 600036, India

(Presented 17 November 2010; received 1 September 2010; accepted 28 November 2010; published online 1 April 2011)

HfO<sub>2</sub> films were produced by sputter deposition in the substrate temperature ( $T_s$ ) range of room temperature (RT)–300 °C and their structural, magnetic, and electrical properties were evaluated. The results indicate that the HfO<sub>2</sub> films crystallize in the monoclinic structure and are oriented along the (–111) direction. Magnetization measurements (300–1.8 K) evidence their RT ferromagnetism. The effect of  $T_s$  is significant on the magnetic moment ( $M$ ) and coercivity ( $H_c$ ).  $M$  and  $H_c$  values enhanced with increasing  $T_s$  due to formation of oxygen vacancies. Increase in the temperature from 150 to 300 K decreases  $H_c$  without any transition, indicating that the Curie temperature of HfO<sub>2</sub> films is higher than RT. Electrical measurements indicate that the HfO<sub>2</sub> films are semiconducting. © 2011 American Institute of Physics. [doi:10.1063/1.3559490]

Hafnium oxide (HfO<sub>2</sub>) is a high temperature refractory material with excellent physical, electronic, and chemical properties.<sup>1–7</sup> The outstanding chemical stability, electrical and mechanical properties, high dielectric constant (high  $k$ ), and wide bandgap of HfO<sub>2</sub> make it suitable for several industrial applications in the fields of electronics, magnetoelectronics, structural ceramics, and optoelectronics.<sup>1–3</sup>

Recently, unexpected ferromagnetism in HfO<sub>2</sub> has been reported by several authors.<sup>6–9</sup> In an ionic configuration, the Hf<sup>4+</sup> ion has a closed shell configuration of [Xe] 4f (Ref. 11) and, consequently, it is nonmagnetic. Theoretical models based on vacancy-induced mechanisms predict that cation vacancies in HfO<sub>2</sub> can exhibit a high-spin state with an associated magnetic moment as large as 4  $\mu_B$ .<sup>6–9</sup> Coey *et al.*<sup>6,7</sup> and Hong *et al.*<sup>8</sup> have attributed the ferromagnetism in HfO<sub>2</sub> to the phenomenon of so-called “ $d^0$  magnetism.” Pemmaraju and Sanvito<sup>10</sup> have demonstrated that intrinsic point defects at Hf sites in HfO<sub>2</sub> films are most likely the source, which could form high-spin defect states, and therefore they could be ferromagnetically coupled with a rather short-range magnetic interaction resulting in a ferromagnetic ground state.

The combination of ferromagnetism with the dielectric characteristics of HfO<sub>2</sub> should enable the integration of metal-oxide semiconductors with spintronics technology.<sup>11–13</sup> The present work was performed on structure and magnetic properties of HfO<sub>2</sub> films from a different perspective. HfO<sub>2</sub> films were grown by radio-frequency magnetron sputter deposition on *c*-cut sapphire substrates at different temperatures and their magnetic behavior is explored. The effect of temperature and microstructure on the magnetism of HfO<sub>2</sub> films was studied in detail. The impetus is to seek the eventual modifications of the magnetic behavior of the oxygen-deficient HfO<sub>2</sub> films induced by the growth temperature.

Interestingly, we found that the origin of ferromagnetism is due to the effect of oxygen vacancies in the undoped HfO<sub>2</sub> films. The results are presented and discussed in this paper.

HfO<sub>2</sub> films were deposited onto *c*-cut sapphire and silicon (Si) wafers by radio-frequency magnetron sputtering. The substrates were cleaned by RCA cleaning. All the substrates were thoroughly cleaned and dried with nitrogen before introducing them into the vacuum chamber, which was initially evacuated to a base pressure of  $\sim 10^{-6}$  Torr. Hafnium metal target (Plasmaterials Inc.) of 2 in. diameter and 99.95% purity was employed for reactive sputtering. The Hf-target was placed on a 2 in. sputter gun, which is placed at a distance of 8 cm from the substrate. The flow of the Ar and O<sub>2</sub> and their ratio (70:30) was controlled using MKS mass flow meters. The deposition was carried out with a sputtering power of 100 W to obtain  $\sim 90$ -nm-thick HfO<sub>2</sub> films. The samples were deposited at different temperatures ( $T_s$ ) varying from RT to 300 °C. The substrates were heated by halogen lamps and the desired temperature was controlled by Athena X25 controller.

The grown HfO<sub>2</sub> films were characterized by performing structural, magnetic, and electrical measurements. X-ray diffraction (XRD) measurements were performed by using a Bruker D8 Advance x-ray diffractometer. All the measurements were made *ex situ* as a function of  $T_s$ . XRD patterns were recorded using Cu  $K\alpha$  radiation ( $\lambda = 1.54056$  Å) at RT. The coherently diffracting domain size ( $D_{hkl}$ ) was calculated from the integral width of the diffraction lines using the well-known Scherrer's equation after background subtraction and correction for instrumental broadening.<sup>14</sup> Magnetization measurements were carried out from 300 to 1.8 K employing a superconducting quantum interference device magnetometer. Electrical conductivity measurements were carried out at RT employing a LCR meter (HP 4192A).

The XRD patterns of HfO<sub>2</sub> films are shown in Fig. 1. It is evident from the XRD patterns that the grown HfO<sub>2</sub> films

<sup>a)</sup>Author to whom correspondence should be addressed. Electronic mail: kbkaruppanan@utep.edu.

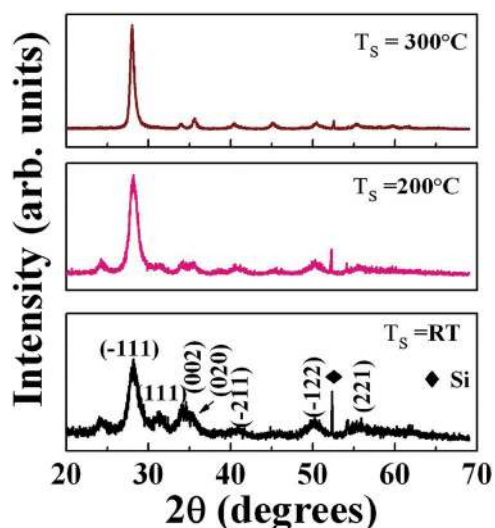


FIG. 1. (Color online) XRD patterns of HfO<sub>2</sub> films grown at various substrate temperatures. HfO<sub>2</sub> films grown at room temperature exhibit the monoclinic phase as indexed. Increasing temperature results in the formation of (−111) oriented structure of monoclinic HfO<sub>2</sub> films.

are polycrystalline. The peaks can be unambiguously assigned to monoclinic HfO<sub>2</sub> phase as labeled (Fig. 1). The peak at 28.1° corresponds to diffraction from (−111) planes. The very broad peak for HfO<sub>2</sub> films grown at RT indicates the presence of nanoparticles. The x-ray peak intensity at 28.1° increases with increasing  $T_s$ , which is indicative of an increase in the average crystallite-size and preferred orientation along (−111). The average crystal dimensions determined from XRD are in the range of 5–24 nm for HfO<sub>2</sub> films grown at  $T_s = RT - 300^\circ\text{C}$ .

The magnetization curves obtained at 300 K are shown in Fig. 2. The curves obtained for the bare substrate and HfO<sub>2</sub> films grown at  $T_s = RT - 300^\circ\text{C}$ . The magnetization curves obtained for HfO<sub>2</sub> samples, before subtraction of the linear diamagnetic background, exhibit weak ferromagnetic signals, which are overlapped on the linear diamagnetic background. Magnetization curves of HfO<sub>2</sub> films obtained after subtracting the background are shown in Fig. 3. The  $M-H$  curves for the HfO<sub>2</sub> films indicate a typical behavior of the ferromagnetism. It is evident that the magnetic moment ( $M \sim 20 \text{ emu/cm}^3$ ) and coercivity  $H_c$  (from 22 to 115 Oe) of the films increases considerably with increasing  $T_s$ .

Zunger *et al.*<sup>15</sup> and Osorio-Guillén *et al.*<sup>16</sup> have reported that the point defects in insulators can create localized levels in the bandgap capable of having different electron occupancies and thus different charge states and magnetic moments. The cation vacancy in four-valent HfO<sub>2</sub> oxide creates a four-hole center for the charge neutral center  $V^0_{\text{cation-IV}}$  and a fully occupied level for the quadruply negative  $V^{4-}_{\text{cation-IV}}$  center. Such partially occupied orbitals (open shell) may give rise to local magnetic moments. For example,  $\mu = 2 \mu_B$  for  $V^0_{\text{cation-II}}$ ,  $\mu = 1 \mu_B$  for  $V^-_{\text{cation-II}}$ , and  $\mu = 4 \mu_B$  for  $V^0_{\text{cation-IV}}$ .

Tirosch and Markovich<sup>17</sup> have reported the RT ferromagnetism in HfO<sub>2</sub> nanorods and attributed the origin of ferromagnetism to the defects. The high magnetic anisotropy found by Coey *et al.* in the thin films and the high magnetic anisotropy of the HfO<sub>2</sub> nanorods reflected through their

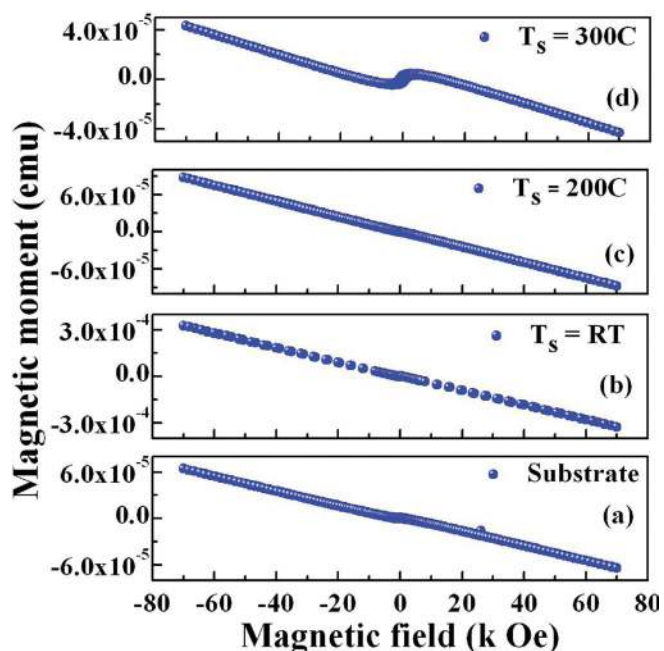


FIG. 2. (Color online) Magnetization curves (at 300 K) of (a) blank sapphire substrate and that of HfO<sub>2</sub> film grown at (b) RT, (c) 200°C, and (d) 300°C, before subtraction of the linear diamagnetic background.

relatively large coercivity can be explained by an anisotropic distribution of defects with respect to the nanorod structure.

In the present case, although a detailed account of experimental probing of the origin of ferromagnetism is not available at this time, ferromagnetic behavior of HfO<sub>2</sub> is clearly seen in the films grown at  $T_s = 300^\circ\text{C}$ . Perhaps, the formation of structural defects and, hence, the defect-induced ferromagnetism may be responsible for the observed magnetic

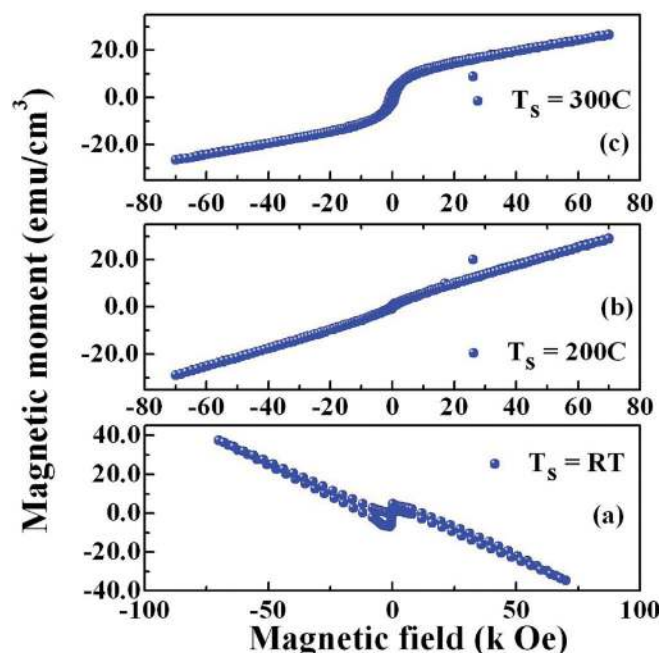


FIG. 3. (Color online) Magnetization curves at 300 K of HfO<sub>2</sub> films grown at (a) RT, (b) 200°C, and (c) 300°C after subtracting the diamagnetic background.

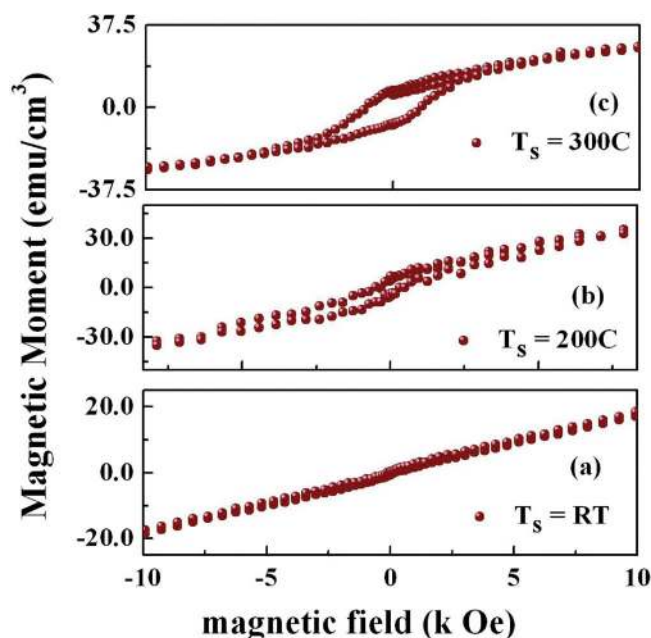


FIG. 4. (Color online) Magnetization curves (at 80 K) of  $\text{HfO}_2$  films grown at (a) RT, (b)  $200^\circ\text{C}$ , and (c)  $300^\circ\text{C}$  after subtracting the diamagnetic background.

behavior of  $\text{HfO}_2$  films.<sup>18</sup> In addition, the presence of oxygen vacancies has been reported for the  $\text{HfO}_2$  films grown by RF sputtering technique with Ar and  $\text{O}_2$  ratio 70:30, where the ferromagnetism is observed.<sup>9</sup> Therefore, in the present case, films are grown with the Ar and  $\text{O}_2$  ratio of 70:30 and at  $T_s = 300^\circ\text{C}$  are expected to form the oxygen-deficient  $\text{HfO}_2$  films. Monoclinic  $\text{HfO}_2$  contains oxygen sites that are surrounded by three or four Hf ions. At higher  $T_s$ , oxygen vacancy and defects could increase, resulting in the creation of localized levels in the bandgap capable of having different electron occupancies and thus different charge states and magnetic moments. It is evident that  $M$  increases with  $T_s$ . Therefore, in the present case, observed ferromagnetism in  $\text{HfO}_2$  films is purely intrinsic and strongly depends on the amount of oxygen vacancy.

Magnetization curves of  $\text{HfO}_2$  films, after background subtraction, at 80 and 1.8 K are shown in Figs. 4 and 5. An increase in  $M$  and  $H_c$  with increasing  $T_s$  is clearly seen from the  $M$ - $H$  curves at 80 and at 1.8 K.

The results of magnetic property measurements indicate that the  $\text{HfO}_2$  films grown at  $T_s = 300^\circ\text{C}$  exhibit the best ferromagnetic behavior compared to other films. The temperature variation of  $M$  from 150 to 300 K for  $\text{HfO}_2$  films grown at  $T_s = 300^\circ\text{C}$  is shown in Fig. 5(d). It is evident that  $M$  decreases continuously with increasing temperature without any transition. We, therefore, conclude that these  $\text{HfO}_2$  films are ferromagnetic at RT with  $T_c$  much higher than 300 K.

The electrical conductivity ( $\sigma$ ) values of  $\text{HfO}_2$  films measured at RT exhibit  $\sigma \sim 10^{-3} (\Omega\text{cm})^{-1}$  indicating their semiconducting nature.  $\sigma$  increases with increasing  $T_s$ .  $\sigma$  increase can be attributed to the increasing crystalline nature and preferred orientation of the film along  $(-111)$ .

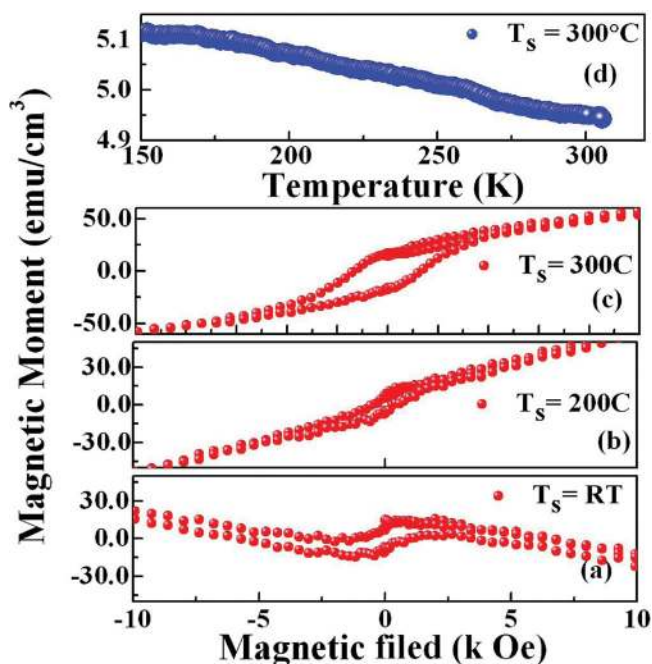


FIG. 5. (Color online) Magnetization curves (at 1.8 K) of  $\text{HfO}_2$  films grown at (a) RT, (b)  $200^\circ\text{C}$ , and (c)  $300^\circ\text{C}$  after subtracting the diamagnetic background. (d) Temperature variation of magnetic moment of the  $\text{HfO}_2$  film grown at  $300^\circ\text{C}$ .

$\text{HfO}_2$  films were fabricated using sputter deposition under varying substrate temperatures in the range of RT– $300^\circ\text{C}$ . The grown  $\text{HfO}_2$  films are polycrystalline, crystallize in monoclinic structure, and orient along the  $(-111)$  direction with increasing  $T_s$ . RT electrical conductivity of  $\text{HfO}_2$  films [ $\sim 10^{-3} (\Omega\text{cm})^{-1}$ ] indicate their semiconducting nature. Magnetization measurements at 300–1.8 K indicate that the  $\text{HfO}_2$  films are ferromagnetic. The magnetic moment and coercivity increases considerably with increasing  $T_s$ . Higher  $T_s$  induce oxygen vacancies and hence the vacancy-induced ferromagnetism in  $\text{HfO}_2$  films. Temperature dependence reveals a decrease in  $M$  with increasing temperature from 150 to 300 K without any transition, indicating that the Curie temperature of  $\text{HfO}_2$  films is higher than the room temperature.

<sup>1</sup>G. D. Wilk *et al.*, *J. Appl. Phys.* **89**, 5243 (2001).

<sup>2</sup>N. Miyata *et al.*, *J. Appl. Phys.* **107**, 103536 (2010).

<sup>3</sup>D. Munoz Ramo *et al.*, *Phys. Rev. Lett.* **99**, 155504 (2007).

<sup>4</sup>A. I. Kingdom *et al.*, *Nature (London)* **406**, 1032 (2000).

<sup>5</sup>P. Boher *et al.*, *Mater. Sci. Eng., B* **109**, 64 (2004).

<sup>6</sup>M. Venkatesan *et al.*, *Nature (London)* **430**, 630 (2004).

<sup>7</sup>J. M. D. Coey *et al.*, *Phys. Rev. B* **72**, 024450 (2005).

<sup>8</sup>N. H. Hong *et al.*, *Phys. Rev. B* **73**, 132404 (2006).

<sup>9</sup>J. Ra and Z. Ya, *J. Semicond. Technol. Sci.* **30**, 102002 (2009).

<sup>10</sup>C. D. Pemmaraju and S. Sanvito, *Phys. Rev. Lett.* **94**, 217205 (2005).

<sup>11</sup>I. Zutic *et al.*, *Rev. Mod. Phys.* **76**, 323 (2004).

<sup>12</sup>G. Prathiba *et al.*, *Solid State Commun.* **150**, 1436 (2010).

<sup>13</sup>J. M. D. Coey, *Solid State Sci.* **7**, 660 (2005).

<sup>14</sup>B. D. Cullity, *Elements of X ray diffraction*, Addison-Wesley Publishing Company, Inc. 1956.

<sup>15</sup>A. Zunger *et al.*, *Physics* **3**, 53 (2010).

<sup>16</sup>J. Osorio-Guillén *et al.*, *Phys. Rev. B* **75**, 184421 (2007).

<sup>17</sup>E. Tirosh and G. Markovich, *Adv. Mater.* **19**, 2608 (2007).

<sup>18</sup>N. H. Hong *et al.*, *Appl. Phys. Lett.* **89**, 042503 (2006).